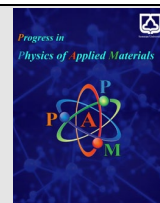




Semnan University

journal homepage: <https://ppam.semnan.ac.ir/>

Investigating the Nonlinear Optical Behavior of $\text{La}_{1-x}\text{Ca}_x\text{Co}_{0.5}\text{Mg}_{0.5}\text{O}_3$ Perovskites

Yasser Rajabi^{a*}, Ahmad Gholizadeh^a, Mahdiyeh Gorzoddin^a^a School of Physics, Damghan University (DU), Damghan, Iran

ARTICLE INFO

Article history:

Received: 18 November 2024

Revised: 4 January 2025

Accepted: 4 January 2025

Keywords:

Nonlinear Optics;

Diffraction Method;

Perovskites;

Laser Beam Intensity.

ABSTRACT

In this study, we synthesized a series of $\text{La}_{1-x}\text{Ca}_x\text{Co}_{0.5}\text{Mg}_{0.5}\text{O}_3$ perovskites with varying Ca content ($x = 0.00, 0.15, 0.45, 0.75$) using the citrate method, aiming to explore the relationship between magnesium doping and the nonlinear optical (NLO) behavior of the materials. Structural and optical characterizations were carried out, with a focus on the impact of Mg substitution on the diffraction ring patterns observed during NLO measurements. Our results reveal that increasing Mg content leads to significant changes in the nonlinear optical response, with a notable enhancement in NLO properties as Mg concentration rises. This suggests that the modification of the perovskite structure through Mg doping plays a crucial role in tuning its optical properties. Convection and conduction flow are also discussed in this article. It is shown that the nanofluid becomes dominated by one flow over the other after some time. The findings demonstrate the potential of $\text{La}_{1-x}\text{Ca}_x\text{Co}_{0.5}\text{Mg}_{0.5}\text{O}_3$ perovskites as promising materials for applications in nonlinear optics and photonic devices, where compositional control can be used to optimize performance.

1. Introduction

The emergence of nanotechnology has revolutionized many fields, providing new materials with properties that differ significantly from their bulk counterparts [1-3]. Among these, nano-perovskites have attracted considerable attention due to their distinctive optical, electronic, and mechanical characteristics, making them prime candidates for a wide array of advanced applications [4,5]. The perovskite crystal structure, denoted by the general formula ABX_3 , is well-known for its versatility, allowing for the incorporation of various chemical compositions, which in turn permits fine-tuning of material properties [6]. When reduced to the nanoscale, these materials exhibit even more pronounced effects, including quantum confinement, enhanced surface-to-volume ratios, and modified electronic band structures, all of which can be harnessed in nonlinear applications.

Nonlinear optical (NLO) phenomena occur when the response of a material to light is not directly proportional to the light's intensity [7,8]. This field has garnered significant

interest due to its applications in modern optical technologies, including laser systems, optical communication networks, and photonic computing [9]. Nano-perovskites have emerged as a promising class of materials in this domain, exhibiting strong nonlinear optical properties [10]. This is largely attributed to their high polarizability, excellent light absorption characteristics, and the ability to fine-tune their electronic properties through compositional or structural modifications. Furthermore, their exceptional charge-carrier mobilities, low exciton binding energies, and high refractive indices enhance their potential for use in a variety of nonlinear optical applications. One of the most studied nonlinear effects in materials is harmonic generation, where photons interacting with a material are converted to new photons with a different frequency. Nano-perovskites have shown considerable potential in second- and third-harmonic generation due to their unique crystal structures, which allow for phase-matching conditions necessary for efficient harmonic conversion [11]. These properties are particularly beneficial for laser technology, where perovskites could

* Corresponding author. Tel.: +98-915-363-0932

E-mail address: y.rajabi@du.ac.ir

Cite this article as:

Rajabi Y., Gholizadeh A., and Gorzoddin M., 2025. Investigating the Nonlinear Optical Behavior of $\text{La}_{1-x}\text{Ca}_x\text{Co}_{0.5}\text{Mg}_{0.5}\text{O}_3$ Perovskites. *Progress in Physics of Applied Materials*, 5(1), pp.47-62. DOI: [10.22075/PPAM.2025.35937.1123](https://doi.org/10.22075/PPAM.2025.35937.1123)© 2025 The Author(s). Progress in Physics of Applied Materials published by Semnan University Press. This is an open-access article under the CC-BY 4.0 license. (<https://creativecommons.org/licenses/by/4.0/>)

enable the development of highly efficient, tunable light sources. Nano-perovskites exhibit saturable absorption, a nonlinear optical property where a material becomes increasingly transparent at high light intensities [12]. This characteristic is critical for applications such as mode-locking in lasers, where nano-perovskite-based saturable absorbers can be employed to produce ultra-short pulses of light [13]. Due to their wide bandgap tunability, nano-perovskites offer flexibility in designing absorbers for specific wavelength ranges, further enhancing their application potential in this domain. The nonlinear optical properties of nano-perovskites make them attractive for a variety of cutting-edge applications [14-16]. In telecommunications, their fast optical response and tunable refractive indices position them as promising candidates for all-optical switches and modulators, which are essential for increasing the bandwidth and efficiency of modern communication networks. In laser technology, their ability to support harmonic generation, saturable absorption, and other nonlinear effects offers the potential to develop more efficient, tunable, and compact laser systems. In bio-imaging and medical diagnostics, nano-perovskites' two-photon absorption properties enable the development of advanced imaging techniques with higher resolution and deeper tissue penetration. Additionally, nano-perovskites hold promise in energy-efficient photonic devices. Their ability to harness nonlinear optical effects could lead to breakthroughs in the development of low-threshold optical switching and energy-saving display technologies. As these materials can be synthesized in a cost-effective manner using solution-based processes, they also present a viable pathway for scalable manufacturing, further driving down costs and expanding their use in commercial applications [14].

In this study, we synthesized a series of $\text{La}_{1-x}\text{Ca}_x\text{Co}_{0.5}\text{Mg}_{0.5}\text{O}_3$ perovskites using the citrate method, with varying Ca content ($x = 0.15, 0.45, \text{ and } 0.75$). The inclusion of magnesium in these perovskite structures is expected to influence their optical and electronic properties, particularly in the context of their nonlinear optical (NLO) behavior. By systematically varying the Ca content, we aim to investigate how the substitution of La with Ca alters the electronic structure and the nonlinear optical response of the material. Special emphasis is placed on understanding the relationship between the Ca content and the observed diffraction rings, a key indicator of NLO behavior, to elucidate the underlying mechanisms driving the optical modulation in these perovskite systems. This study contributes to the broader understanding of how compositional changes in perovskites can be leveraged to tune their optical properties for potential applications in photonics and nonlinear optical devices.

2. Experimental Procedure

The $\text{La}_{1-x}\text{Ca}_x\text{Co}_{0.5}\text{Mg}_{0.5}\text{O}_3$ perovskites with Ca content ($x = 0.15, 0.45, 0.75$) were synthesized using the citrate method with metal nitrate precursors in the presence of citric acid [6]. Initially, an aqueous solution was prepared containing appropriate concentrations of La $(\text{NO}_3)_3 \cdot 6\text{H}_2\text{O}$,

$\text{Ca}(\text{NO}_3)_2 \cdot 4\text{H}_2\text{O}$, $\text{Mg}(\text{NO}_3)_2 \cdot 2\text{H}_2\text{O}$, $\text{Co}(\text{NO}_3)_2 \cdot 6\text{H}_2\text{O}$, and citric acid, with the latter being in an amount equivalent to the total moles of nitrate ions present. This solution was evaporated at 60°C overnight, resulting in a homogenous sol-like substance. The sol was then dried at 80°C overnight, yielding a spongy, friable material that was subsequently powdered and heated at 200°C overnight to form the precursor. To eliminate carbonaceous material, the precursor was calcined at 600°C for 5 hours. The resulting powder was ground and sintered at 900°C for 5 hours to obtain the final perovskite products.

X-ray diffraction (XRD) patterns were recorded using a Bruker AXS D8 ADVANCE diffractometer (Bruker-AXS, Karlsruhe, Germany) with $\text{CuK}\alpha$ radiation over a 2θ range of 20° – 80° at room temperature. The data were analyzed using the X'pert package and the Foolproof program. The crystallite sizes of the samples were calculated using the Scherrer equation. In this method, the broadening of the XRD peaks is attributed to the crystallite size. The full width at half-maximum (FWHM) of the diffraction peak near $2\theta \approx 47^\circ$ was used in the calculation. Instrumental broadening was subtracted by using undeformed silicon as a standard reference material, allowing accurate determination of the broadening effects attributed solely to the sample.

3. Nonlinear Optical Behavior in Nano-Perovskites

Nonlinear optics describes the interaction of high-intensity light with materials, where the response of the material becomes nonlinear with respect to the electric field of the light [7]. This can result in phenomena such as Second-harmonic generation (SHG), Third-harmonic generation (THG), Self-focusing, Self-phase modulation, Nonlinear refractive index changes (Kerr effect). Nano-perovskites (especially transition metal oxides like $\text{La}_{1-x}\text{Ca}_x\text{Co}_{0.5}\text{Mg}_{0.5}\text{O}_3$) often exhibit unique electronic and optical properties due to their reduced dimensions, quantum confinement, and modified surface states. The doping of calcium (Ca) into the $\text{LaCo}_{0.5}\text{Mg}_{0.5}\text{O}_3$ lattice can tune the optical and electronic properties by modifying the bandgap, introducing defects, and altering the electron-lattice interactions. Diffraction rings in the context of nonlinear optics often arise due to self-diffraction phenomena, where the material's nonlinear refractive index causes the laser light to diffract in a ring-like pattern. Various techniques are available to characterize the nonlinear (NL) optical response of materials. Among them are the Z-scan technique, pump-probe spectroscopy, harmonic generation analysis, and diffraction ring pattern analysis [17,18]. These methods enable researchers to investigate the behavior of materials under intense laser irradiation, facilitating the development of advanced technologies in fields such as laser processing, optical communications, and quantum optics. The Z-scan technique measures a material's nonlinear refractive index by moving a focused laser beam through the sample [18]. Pump-probe spectroscopy involves using two synchronized laser pulses to examine the ultrafast dynamics of a material. Harmonic generation analysis

explores the creation of higher harmonic frequencies in response to an incident laser, while diffraction ring pattern analysis studies the rings formed when light interacts with a material. This latter method is particularly valuable for probing the nonlinear optical properties of materials, making it important for applications in photonics and optoelectronics [19].

When a high-power Gaussian laser interacts with a nonlinear medium, it produces far-field diffraction patterns known as Fraunhofer patterns, which consist of concentric rings. The characteristics of these patterns, such as the focal point size and ring spacing, depend on the properties of the optical system [20]. The formation of these rings is due to various physical mechanisms inducing phase shifts on the Gaussian wavefront. These phase shifts cause the distorted re-radiated waves to have different frequencies from the incident wave, allowing the relationship between the material's nonlinear refractive index and the number of rings to be determined.

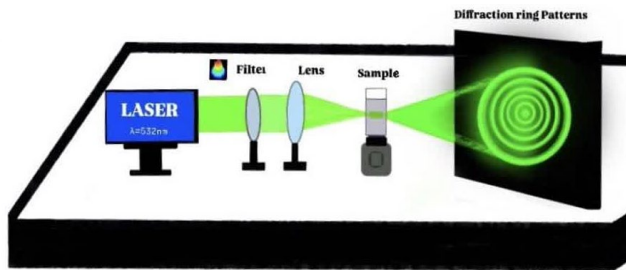


Fig. 1. An experimental setup

In the experimental setup (Fig.1), a continuous-wave diode-pumped solid-state laser, operating at 532 nm, was focused on the sample using a 250 mm focal length lens. The laser beam was carefully directed to ensure optimal illumination of the sample, which was contained in a cell placed between the lens and the focal point. The nano-fluid in the cell, with a path length of 1 mm, was designed to maximize interaction with the laser. A Basler acA640-750uc camera, equipped with an ON-Semiconductor PYTHON 300 CMOS sensor, was used to capture the sample's response to the laser irradiation, recording up to 551 frames per second at VGA resolution. The laser beam had a diameter of 0.5 mm at the sample surface. To ensure effective interaction, the nano-fluid was selected for its high absorption of green light. As the laser passed through the fluid, the beam diverged, producing a series of concentric diffraction rings. These rings were observed on a screen positioned 50 cm from the front of the cell, and their patterns were carefully documented for further analysis.

4. Results and Discussion

Fig. 1 presents the X-ray diffraction (XRD) patterns of $\text{La}_{1-x}\text{Ca}_x\text{Co}_{0.5}\text{Mg}_{0.5}\text{O}_3$ samples with $x = 0.15, 0.45,$ and 0.75 . The XRD data were analyzed using the X'Pert High Score package. Structural analysis confirmed the presence of an orthorhombic perovskite phase in $x = 0.15$. The XRD pattern of $x = 0.45$ is a mixture of two phases orthorhombic

and rhombohedral. It should be noted that the diffraction pattern is typical; when varying the Ca content, a ratio of the orthorhombic and rhombohedral phases changes only; the lines with largest intensity of both phases coincide. In the XRD patterns of $x = 0.75$, slight peak splitting observed around $33^\circ, 41^\circ, 58^\circ, 68^\circ,$ and 78° suggests a rhombohedral structure. However, the XRD patterns reveal the occurrence of structural phase transitions, indicating that different structures are present depending on the Ca content.

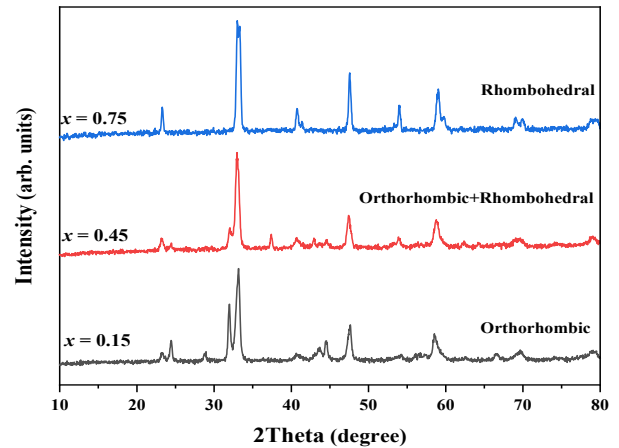


Fig. 2. X-ray diffraction patterns of $\text{La}_{1-x}\text{Ca}_x\text{Co}_{0.5}\text{Mg}_{0.5}\text{O}_3$ catalyst

Fig. 3 illustrates the temporal evolution of far-field diffraction patterns of a high-power laser beam passing through nanofluid with a manganese concentration of 0.75 at different power levels. The diffraction rings were recorded at various incident laser powers. Fig. 3a corresponds to a power of 147 mW, Fig. 3b to 100 mW, Fig. 3c to 58 mW, and Fig. 3d to 17 mW. The results clearly demonstrate that the nonlinear optical behavior of the sample varies with different incident laser intensities. Additionally, the findings indicate that the sample exhibits better nonlinear optical behavior at higher power levels compared to lower ones. In Fig. 3, it can be observed that over time, the number of diffraction rings increases. At a certain point, the number of rings stabilizes ($t=105$ ms). By counting the number of rings (N), the nonlinear refractive index of the sample by following equation, can be determined [20]:

$$\Delta n = \frac{N\lambda}{L} \quad (1)$$

$N, \lambda,$ and L are the number of diffraction rings, wavelength of laser beam, and thickness sample respectively. Also Δn is [20]:

$$\Delta n = n_2 I \quad (2)$$

where n_2 is the nonlinear refractive index.

As shown in the figure, at later times, the number of diffraction rings no longer increases; instead, the radius of the ring's changes in both horizontal and vertical directions. This phenomenon is known as the collapse effect. Prior to the collapse time, the radius remains equal in both directions, indicating that conductive currents in the fluid dominate over

convective currents. However, after the collapse time, convective currents become dominant over conductive ones.

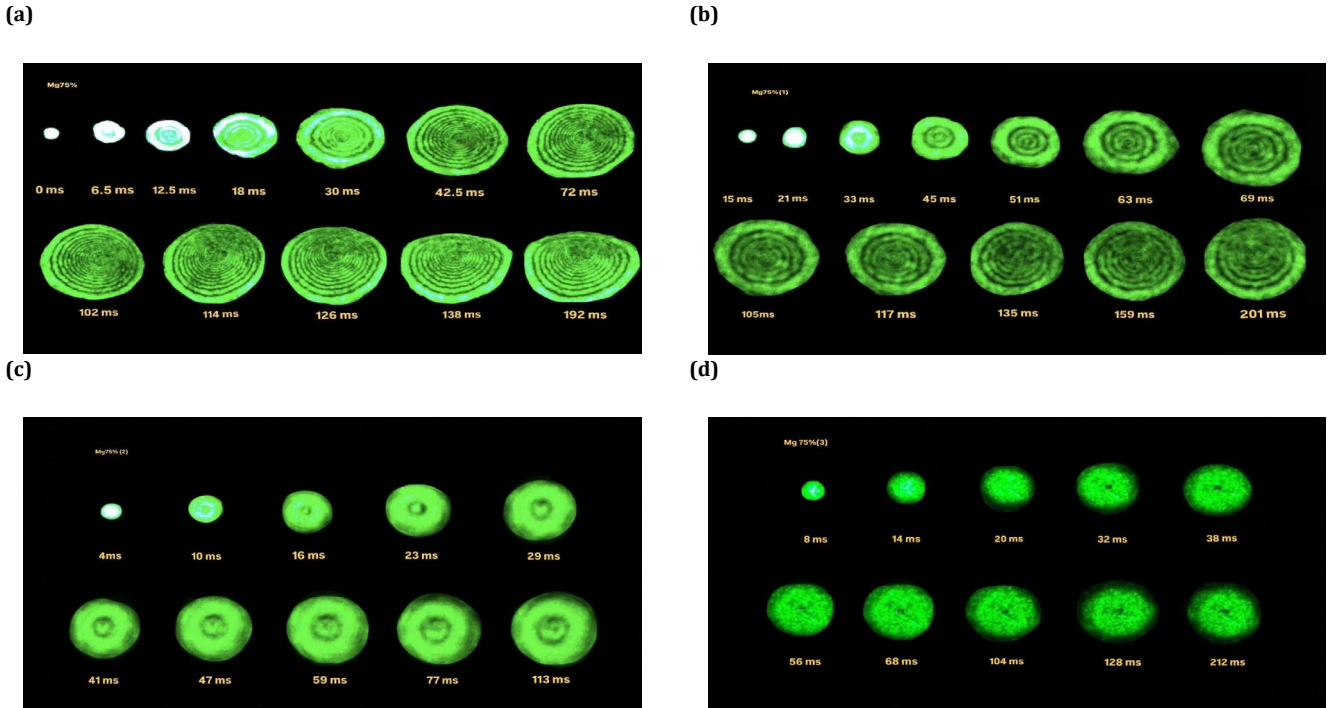


Fig. 3. Images of the temporal evolution of the far-field diffraction pattern of a laser beam passing through the liquid sample for $x=0.75$, and (a) $p=147\text{mW}$, (b) $p=100\text{mW}$, (c) $p=58\text{mW}$, and (d) $p=17.8\text{mW}$

Fig. 4 shows samples of the temporal evolution of diffraction rings for a magnesium concentration of 0.45 at

different power input of the high-intensity laser beam on the nanofluid.

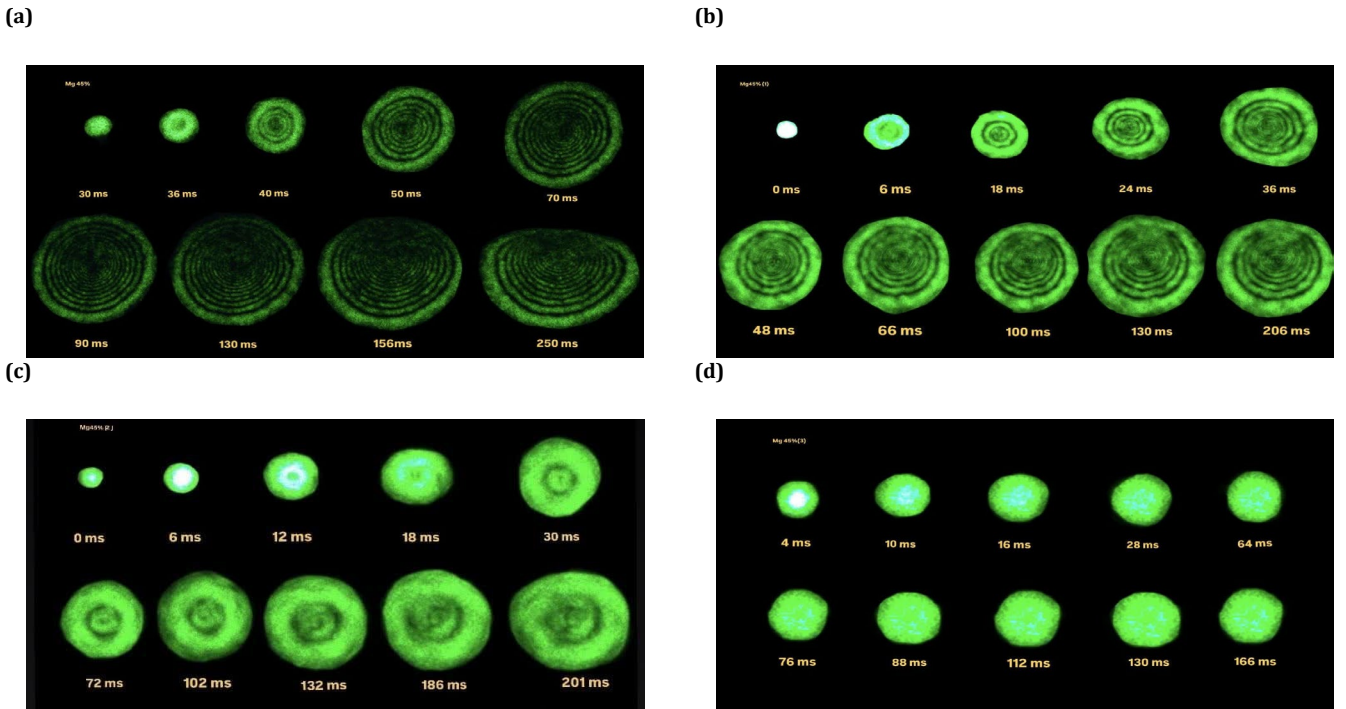


Fig. 4. Shows the temporal evolution of one diffraction ring pattern for nanofluid with $x=0.45$, and for different input power of (a) $p=147\text{mW}$, (b) $p=100\text{mW}$, (c) $p=58\text{mW}$, (d) $p=17.8\text{mW}$

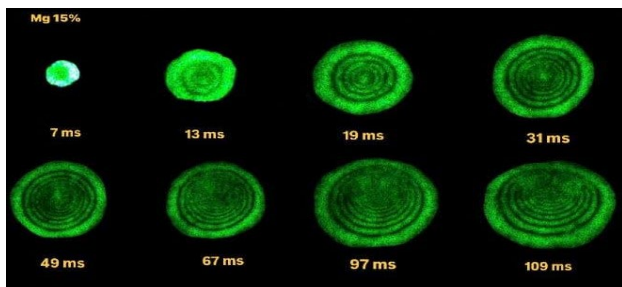
As the intensity of the incident beam increases, the diffraction rings lose their symmetry in the vertical

direction compared to the horizontal. Fig. 4a shows the temporal evolution of the diffraction rings, where the

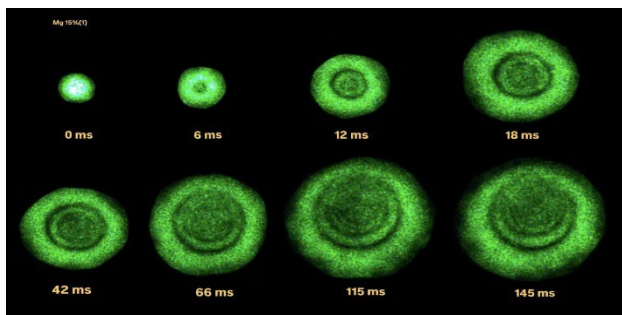
transformation begins from a single spot point ($t = 0$ s) and subsequently changes into full circular rings ($t = 130$ ms) and then into elliptical shapes ($t = 150$ ms) and so on as time lapse due to convection effects. Fig. 4b shows the temporal evolution of diffraction rings at a power of 100 mW. In this figure, the temporal evolution also begins from a single spot point ($t = 0$ s) and progresses to a complete full circular ring ($t = 130$ ms). It is clearly observed that, unlike the temporal evolution of diffraction rings at an incident laser power of 147 mW, the diffraction rings do not transform into an elliptical shape or experience the dominance of convection flow. Fig. 4c and 4d show the temporal evolution of diffraction rings at powers of 58 and 17.8 mW. The results clearly demonstrate that with a reduction in power, no transformation in the diffraction rings is observed. Consequently, at these power levels, no nonlinear optical behavior is observed in this nanofluid.

The temporal evolution of far-field diffraction rings for the perovskite sample with a manganese concentration of 0.15 is shown in Fig. 5.

(a)



(b)



(c)

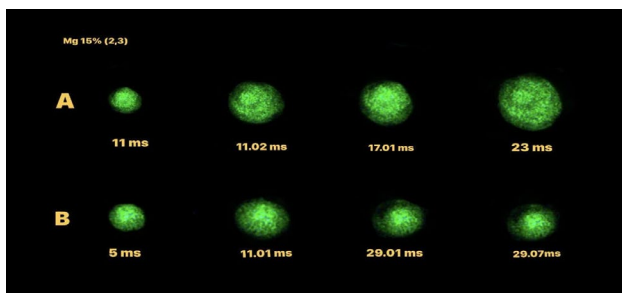


Fig. 5. Images of the temporal evolution of the far-field diffraction pattern of a laser beam passing through the liquid sample for $x=15$, and (a) $p=147$ mW, (b) $p=100$ mW, (c) $p=58$ mW, and (d) $p=17.8$ mW

Fig. 5a and 5b show the temporal evolution of diffraction rings at two intensities, 147 and 100 mW. In these figures, the formation of rings is clearly demonstrated. However, Figure 5b shows no transformation from circular to elliptical rings.

Fig. 5c simultaneously shows the temporal evolution of diffraction rings at two intensities, 50 and 17 mW. As observed, no rings are seen at these power levels. This result indicates that the 0.15 sample does not exhibit nonlinear behavior at intensities of 50 and 17 mW.

The captured observed diffraction rings were accounted for from the obtained figures. Then, all the nonlinear refractive indices (n_2) are obtained by using Eq. 1. Its calculated values for n_2 are shown in Table 1.

Table 1. The calculated NL optical parameters

	Laser intensity ($\times 10^{+9} W/m^2$)	Ca concentration			$n_2 (\times \frac{10^{-12} m^2}{W})$		
		0.75	0.45	0.15	0.75	0.45	0.15
1	1.3	15	10	8	6.14	4	3.2
2	0.88	7	6	3	3	2.4	1.2
3	0.44	5	3	1	2	1.2	0.4
4	0.15	3	0	0	1.2	0	0

The comparison of the number of diffraction rings with the manganese concentration amount in different laser power intensity is illustrated in Fig. 6, where a clear correlation is observed.

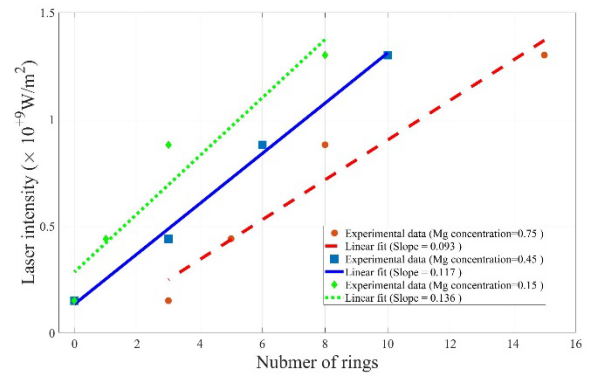


Fig. 6. Variation of the No. Of diffraction rings concerning the incident laser power intensity

In Fig. 6, the relationship between the intensity of the incident beam and the number of far-field diffraction rings for samples with different magnesium concentrations is illustrated. According to the graph, the number of diffraction rings is higher for the sample with the highest magnesium concentration (0.75), shown in red on the graph. It is also observed that at an intensity of 17 mW, diffraction rings are not visible for the concentrations of 0.15 and 0.45, indicating the absence of nonlinear behavior in these samples at this intensity. This finding suggests that the 0.75 concentration exhibits the strongest nonlinear behavior at an intensity of 147 mW. Additionally, it is evident that as the magnesium concentration decreases, the nonlinear behavior also diminishes.

5. Conclusions

In this study, a series of nano-perovskites with varying magnesium concentrations were synthesized using the citrate method. Far-field diffraction rings were observed as a result of the propagation of a high-power laser beam. These observations clearly demonstrate that the synthesized nano-perovskites exhibit nonlinear optical properties. The results also indicate that the nonlinear optical behavior of the nano-perovskites changes with the intensity of the incident beam. Furthermore, altering the magnesium concentration in the nano-perovskites affects their nonlinear optical response. These characteristics make this sample a strong candidate for applications in nonlinear optics and optoelectronics, with potential uses across various fields related to nonlinear optics.

Conflicts of interest

The author declares that there is no conflict of interest regarding the publication of this article.

References

- [1] Gholizadeh, A. and Hosseini, S., 2024. Effect of heavy rare-earth substitution on physical properties of BiFeO₃ thin films and their photocatalytic application. *Journal of the American Ceramic Society*, 107(6), pp.4209-4222.
- [2] Panconi, L., Euchner, J., Tashev, S.A., Makarova, M., Herten, D.P., Owen, D.M. and Nieves, D.J., 2024. Mapping membrane biophysical nano-environments. *Nature Communications*, 15(1), p.9641.
- [3] Lee, H., Kim, S., Eom, S., Ji, G., Choi, S.H., Joo, H., Bae, J., Kim, K.K., Kravtsov, V., Park, H.R. and Park, K.D., 2024. Quantum tunneling high-speed nano-excitonic modulator. *Nature Communications*, 15(1), p.8725.
- [4] Zanetta, A., Larini, V., Vikram, Toniolo, F., Vishal, B., Elmestekawy, K.A., Du, J., Scardina, A., Faini, F., Pica, G. and Pirota, V., 2024. Vertically oriented low-dimensional perovskites for high-efficiency wide band gap perovskite solar cells. *Nature communications*, 15(1), p.9069.
- [5] Nowok, A., Sobczak, S., Roszak, K., Szeremeta, A.Z., Mączka, M., Katrusiak, A., Pawlus, S., Formalik, F., Barros dos Santos, A.J., Paraguassu, W. and Sieradzki, A., 2024. Temperature and volumetric effects on structural and dielectric properties of hybrid perovskites. *Nature communications*, 15(1), p.7571.
- [6] Gholizadeh, A., 2017. La_{1-x}Co_{1-y}Mg_yO₃ nano-perovskites as CO oxidation catalysts: Structural and catalytic properties. *Journal of the American Ceramic Society*, 100(3), pp.859-866.
- [7] Yildirim, M., Dinc, N.U., Oguz, I., Psaltis, D. and Moser, C., 2024. Nonlinear processing with linear optics. *Nature Photonics*, 18(10), pp.1076-1082.
- [8] Sekikawa, T., Kosuge, A., Kanai, T. and Watanabe, S., 2004. Nonlinear optics in the extreme ultraviolet. *Nature*, 432(7017), pp.605-608.
- [9] Alizadeh, A., Rajabi, Y. and Bagheri-Mohagheghi, M.M., 2022. Effect of crystallinity on the nonlinear optical properties of indium-tin oxide thin films. *Optical Materials*, 131, p.112589.
- [10] Guan, Z., Fu, L., Wei, Z., Shan, N., Li, H., Fang, Y., Zhao, Y., Huang, Z., Humphrey, M.G. and Zhang, C., 2023. Toward strong nonlinear optical absorption properties of perovskite films via porphyrin axial passivation. *Materials Today Physics*, 35, p.101135.
- [11] Shen, W., Chen, J., Wu, J., Li, X. and Zeng, H., 2020. Nonlinear optics in lead halide perovskites: mechanisms and applications. *Acs Photonics*, 8(1), pp.113-124.
- [12] Wei, Q., Wang, C. and Li, M., 2023. Halide perovskite micro and nano lasers. In *Metal Halide Perovskites for Generation, Manipulation and Detection of Light* (pp. 219-255). Elsevier.
- [13] Zhang, Q., Shang, Q., Su, R., Do, T.T.H. and Xiong, Q., 2021. Halide perovskite semiconductor lasers: materials, cavity design, and low threshold. *Nano Letters*, 21(5), pp.1903-1914.
- [14] Rashid, A. and Ikram, M., 2024. Optical characterization of La₂SrFe₂TiO₉ triple perovskite: Insights for advanced optoelectronic and solar cell applications. *Optik*, 308, p.171843.
- [15] Liu, X., Wang, Y., Wang, Y., Zhao, Y., Yu, J., Shan, X., Tong, Y., Lian, X., Wan, X., Wang, L. and Tian, P., 2022. Recent advances in perovskites-based optoelectronics. *Nanotechnology Reviews*, 11(1), pp.3063-3094.
- [16] Zhou, Y., Huang, Y., Xu, X., Fan, Z., Khurgin, J.B. and Xiong, Q., 2020. Nonlinear optical properties of halide perovskites and their applications. *Applied Physics Reviews*, 7(4).
- [17] Sheik-Bahae, M., Said, A.A. and Van Stryland, E.W., 1989. High-sensitivity, single-beam n² measurements. *Optics letters*, 14(17), pp.955-957.
- [18] Gheymasi, A.N., Rajabi, Y. and Zare, E.N., 2020. Nonlinear optical properties of poly (aniline-co-pyrrole) @ ZnO-based nanofluid. *Optical Materials*, 102, p.109835.
- [19] R. Boyd, *Nonlinear Optics*, 3rd Edition, ISBN: 9780080485966, Academic Press, 1-640, 2008.
- [20] Karimzadeh, R., 2013. Studies of spatial self-phase modulation of the laser beam passing through the liquids. *Optics communications*, 286, pp.329-333.